Reactive oxygen species mediated apoptosis of esophageal cancer cells induced by marine triprenyl toluquinones and toluhydroquinones

Catherine E. Whibley,[1] Kerry L. McPhail,[2] Robert A. Keyzers,[2] Michelle F. Maritz,[1] Virna D. Leaner,[1] Michael J. Birrer,[3] Michael T. Davies-Coleman,[2] and Denver T. Hendricks[1]

[1]Institute of Infectious Diseases and Molecular Medicine, Division of Medical Biochemistry, University of Cape Town, Faculty of Health Sciences, Cape Town, South Africa; [2]Department of Chemistry, Rhodes University, Grahamstown, South Africa; and [3]Cell and Cancer Biology Branch, Center for Cancer Research, National Cancer Institute, Bethesda, Maryland

Abstract

Marine invertebrates, algae, and microorganisms are prolific producers of novel secondary metabolites. Some of these secondary metabolites have the potential to be developed as chemotherapeutic agents for the treatment of a wide variety of diseases, including cancer. We describe here the mechanism leading to apoptosis of esophageal cancer cell lines in the presence of triprenylated toluquinones and toluhydroquinones originally isolated from the Arminacean nudibranch *Leminda millecra*. Triprenylated toluquinone–induced and toluhydroquinone-induced cell death is mediated via apoptosis after a cell cycle block. Molecular events include production of reactive oxygen species (ROS), followed by induction and activation of c-Jun (AP1) via c-Jun-NH_2-kinase–mediated and extracellular signal-regulated kinase–mediated pathways. Partial resistance to these compounds could be conferred by the ROS scavengers Trolox and butylated hydroxyanisol, a c-Jun-NH_2-kinase inhibitor, and inhibition of c-Jun with a dominant negative mutant (TAM67). Interestingly, the levels of ROS produced varied between compounds, but was proportional to the ability of each compound to kill cells. Because cancer cells are often more susceptible to ROS, these compounds present a plausible lead for new antiesophageal cancer treatments and show the potential of the South African marine environment to provide new chemical entities with potential clinical significance. [Mol Cancer Ther 2007;6(9):2535–43]

Introduction

Despite the current focus on new chemical entities generated by combinatorial synthetic programs, natural products (secondary metabolites) still remain an extremely promising reservoir of chemotherapeutic lead compounds, with over 60% of currently used chemotherapeutic agents derived or developed from natural sources (1, 2). Many marine organisms (invertebrates, algae, and microorganisms) produce natural products as a chemical defense against predation or in a response to interspecies competition for limited resources (e.g., space on a reef or nutrients; ref. 3). Interestingly, the isolation and identification of marine natural products by chemists, working in tandem with pharmacologists, over the last three decades has provided important lead compounds for the pharmaceutical industry, especially in the field of new anticancer drug discovery (4–6). Marine biota are a unique reservoir of biomolecular diversity, not only because of the large number of species present in the oceans, but also because the marine environment presents very different physiological and ecological challenges compared with those experienced by terrestrial species. As a consequence of the differences between terrestrial and marine habitats, the initial expectation that marine organisms use unique biosynthetic pathways or exploit variations on established biosynthetic pathways to biosynthesize structurally unusual natural products has been validated by the complexity and novelty of the plethora of marine natural products isolated over the last 30 years (3, 7).

The southern African coastline has the potential to yield many useful compounds, as the high marine invertebrate species endemism in the coastal waters is associated with high secondary metabolite diversity (8). In our laboratory, we test compounds from a variety of sources for activity against squamous esophageal cancer cell lines (9–13). Key among these compounds are the natural products isolated from marine organisms and collected using SCUBA off the southern and east African coast (13). Squamous esophageal cancer cells were selected as a model system because this cancer is one of the most frequent cancers in males in South Africa, with an age standardized incidence rate of 16.22 per 100,000 (14), and is one of the primary causes of cancer-related deaths in South African Black males. Current therapy for esophageal cancer is complicated by the fact that the disease is normally diagnosed late once a large

Received 12/7/06; revised 5/18/07; accepted 8/1/07.

Grant support: Cancer Association of South Africa, South African National Research Foundation, South African Government Department of Environmental Affairs and Tourism, Rhodes University, and University of Cape Town.

The costs of publication of this article were defrayed in part by the payment of page charges. This article must therefore be hereby marked *advertisement* in accordance with 18 U.S.C. Section 1734 solely to indicate this fact.

Requests for reprints: Denver Hendricks, Division of Medical Biochemistry, University of Cape Town, Faculty of Health Sciences, Private Bag X3, Observatory, Cape Town, 7935, South Africa. Phone: 27-21-406-6266; Fax: 27-21-406-6061. E-mail: Denver.Hendricks@uct.ac.za

doi:10.1158/1535-7163.MCT-06-0760

tumor mass is present and begins to obstruct swallowing. Chemotherapy most often consists of a combined cisplatin/5-fluorouracil regimen, and if treatment is initiated at an early stage of the disease, complete remission occurs in 20% to 30% of treated patients (15). However, early diagnosis rarely occurs, and the 5-year survival rate is currently only 14% (16). Because other treatment modalities (radiotherapy and surgery) are not likely to improve this outlook in the near future, there is a need for more effective chemotherapeutic agents to be developed. Cervical cancer cells were included in the screening program because this disease is the leading cause of cancer deaths among women in South Africa, with a total age standardized incidence rate of 31.08 per 100,000, and is especially prevalent among Black women with an age standardized incidence rate of 38.46 per 100,000, one of the highest in the world (14). The high incidence is due to limited screening, and thus, the majority of cases of cervical cancer in South Africa, like esophageal cancer, are only diagnosed at a late stage.

An earlier natural product investigation of metabolites from South African marine organisms yielded a variety of novel chemical compounds from the endemic South African nudibranch *Leminda millecra* (17). The secondary metabolites isolated from *L. millecra* included a group of related triprenyl toluquinones and triprenyl toluhydroquinones, which exhibited similar cytotoxic activity to cisplatin in our culture system. These compounds induced cell cycle arrest and apoptosis in cultured cells, which was related to reactive oxygen species (ROS) production and activation of c-Jun/AP1. The limited yield of these compounds precluded further investigation; however, synthesis of these compounds and analogues is being pursued. Once an adequate supply of synthetic material is available, animal studies to test *in vivo* efficacy and to address the pharmacokinetic properties of these compounds will be done.

This study shows that the Southern African marine environment shows considerable promise as a source of potential chemotherapeutic lead agents for esophageal cancer.

Materials and Methods

Chemicals

The triprenylated toluquinones and toluhydroquinones used in this study were originally isolated from the nudibranch *L. millecra* (17), i.e., 5-methyl-2-[(2′E,6′E)-3′,7′,11′-trimethyl-2′,6′-dodecadien-9′-onyl]benzo-1,4-quinone (KLM153), 5-methyl-2-[(2′E,7′Z)-3′,7′,11′-trimethyl-2′,7′-dodecadien-9′-onyl]benzo-1,4-quinone (KLM154), 5-methyl-2-[(2′E,6′E)-3′,7′,11′-trimethyl-2′,6′-dodecadien-9′-onyl]-1,4-dihydroxybenzene (KLM155), 5-methyl-2-[(2′E,7′Z)-3′,7′,11′-trimethyl-2′,7′-dodecadien-9′-onyl]-1,4-dihydroxybenzene (KLM156), 1-acetoxy-5-methyl-2-[(2′E,7′Z)- 3′,7′,11′-trimethyl-2′,7′-dodecadien-9′-onyl]-4-hydroxybenzene (KLM157), and 5-methyl-2-[(2′E,6′E)-9′-hydroxy-3′,7′,11′-trimethyl-2′s,6′-dodecadienyl]-1,4-dihydroxybenzene (KLM159). All test compounds were suspended in DMSO at 100 mmol/L and stored at −20°C.

Hydrocortisone, epidermal growth factor, doxycyclin hydrochloride, cholera toxin, insulin, propidium iodide, butylated hydroxyanisol, and tocopherol were purchased from Sigma. Crystal violet was purchased from BDH. Cell culture media and supplements were purchased from Highveld Biological. Extracellular signal-regulated kinase (ERK) and β-tubulin antibodies were purchased from Santa Cruz. Phosphorylated p38, phosphorylated ERK, phosphorylated c-Jun-NH_2-kinase and JNK (PhosphoPlus antibody kit 9250), and phosphorylated c-Jun and c-Jun (PhosphoPlus antibody kit 9260) antibodies were purchased from Cell Signaling. p38 antibody was purchased from Sigma. All other chemicals were analytic grade.

Cell Culture and Cell Proliferation Assays

Cells were maintained in a humidified, 37°C, 5% CO_2 incubator. WHCO1 and WHCO6 cells (esophageal cancer cell lines; ref. 18), CaSki cells (a cervical cancer cell line), and TAM67 cells (CaSki cells stably transfected with the c-Jun dominant negative construct TAM67; refs. 19, 20) were cultured in DMEM supplemented with 10% FCS, 100 units/mL penicillin, and 100 μg/mL streptomycin. TAM67 cells were provided as a gift from V. Leaner and M. Birrer and were maintained in media with 5 μg/mL blasticidin. ME180 cells (a cervical cancer cell line) were maintained in McCoy's 5A medium supplemented with 10% FCS, 100 units/mL penicillin, and 100 μg/mL streptomycin. SiHa cells (a cervical cancer cell line) were maintained in MEM, 10% FCS, 100 units/mL penicillin, and 100 μg/mL streptomycin. MCF12F cells (a benign breast epithelial cell line) were maintained in 1:1 DMEM/Hams F12 medium supplemented with 20 ng/mL epidermal growth factor, 0.1 μg/mL cholera toxin, 0.5 μg/mL hydrocortisone, and 10 μg/mL insulin.

Pictures of cells were obtained using a Zeiss Axiovert 200 with an Axiocam camera and Axiovision 4.1 image software.

Crystal violet assays were done as previously described (13). 3-(4,5-Dimethylthiazol-2-yl)-2,5-diphenyltetrazolium bromide (MTT) assays were done using the MTT kit from Roche according to manufacturer's instructions and as previously described (10, 12).

Cell Cycle Analysis

WHCO1 cells were seeded in 60-mm dishes at 0.25×10^6 cells per dish. After an overnight settling period, cells were treated with the indicated concentrations of KLM155. At appropriate time points, cells were harvested (including floating cells) and fixed in 70% ethanol at −20°C for up to 2 weeks. Cells (5×10^6 per mL) were incubated with 50 μg/mL RNase A in PBS for 30 min at room temperature. Staining solution (0.1% Triton X100, 2 mmol/L $MgCl_2$, 100 mmol/L NaCl, 0.01 mol/L PIPES buffer, 10 μg/mL propidium iodide) was added, and cells were analyzed on a Beckman Coulter FACS-calibur flow cytometer. Analysis of cell cycle results was carried out using ModFit 3.0 (Verity Software House).

Apoptosis Assay

Caspase-3 activity in cells was used as a measure of apoptosis and was measured using the Caspase-Glo 3/7

assay kit according to manufacturer's instructions (Promega). Cells were seeded at 1,000 cells per well in 96-well plates in 60 μL. After 24 h incubation to allow cells to settle and, in some cases, a 2-h pretreatment with inhibitors, compounds were added as outlined and cells were incubated for the indicated time periods before processing. Luminescence was detected using a Luminoskan Ascent plate reader.

The induction of apoptosis was confirmed using a flow cytometric approach using a fluorescently labeled antibody to activate caspase-3 according to manufacturer's instructions. Fluorescence was detected using a Beckman Coulter FACS-calibur flow cytometer.

Necrosis Assay

Analysis of the levels of necrosis was done using the CytoTox-ONE homogeneous membrane integrity assay (Promega) according to manufacturer's instructions. At each time point, lysis buffer (supplied with the kit) was added to a set of wells as a positive control. Fluorescence was measured on a 96-well plate fluorimeter, and values were expressed as a percentage of the positive control.

Measurement of ROS

Cells were plated in 60-mm dishes at 5×10^5 cells per dish. After a 24-h incubation, the media was removed, cells rinsed with prewarmed Krebs-Ringer buffer [110 mmol/L NaCl, 2.6 mmol/L KCl, 1.2 mmol/L $MgSO_4$, 1.2 mmol/L KH_2PO_4, 25 mmol/L $NaHCO_3$, 11 mmol/L glucose (pH 7.4)], and 2 mL of 25 μmol/L DCF-DA in Krebs-Ringer buffer was added. After a 15-min incubation at 37°C, 5% CO_2 in the dark, test compound was added and cells were incubated for another hour. Cells were then harvested using trypsin, centrifuged, resuspended in 1 mL Krebs-Ringer buffer, and analyzed by flow cytometry on a FACS-calibur flow cytometer.

Western Blotting

Cells were harvested in 200 μL of radioimmunoprecipitation assay buffer [150 mmol/L NaCl, 1% Triton X100, 0.1% SDS, 10 mmol/L Tris (pH 7.5), 1% deoxycholate] with protease inhibitor (Complete tablets, Roche), and lysates were stored at −20°C. After sonication and protein determination using the Pierce BCA kit, equal amounts of protein were loaded on a 15% polyacrylamide gel and subjected to electrophoresis at 200 V. After transfer at 100 V for 1 h, membranes were stained with Ponceau S to assess protein loading and then blocked with 5% fat-free milk in TBS with 0.1% Tween 20 for 1 h. After incubation with the indicated primary antibody and horseradish peroxidase–conjugated antirabbit or antimouse secondary antibody, detection using either LumiGLO Reserve Chemiluminescent Substrate kit (KPL) or Extended West Dura Super Signal (Pierce) was carried out. Bands were visualized by autoradiography, after which the blots were stripped and reprobed for β-tubulin as a loading control.

Statistical Analysis

Unless otherwise indicated, error bars indicate SD.

For ROS determination, each experimental condition was carried out in triplicate, and results are the mean ± SD and are representative of two or more independent experiments.

Apoptosis experiments and determinations of cell number by MTT assay were carried out in quadruplicate, and results are the mean ± SD and are representative of two or more independent experiments.

Each concentration for IC_{50} determination was tested in quadruplicate, and each IC_{50} determination was repeated

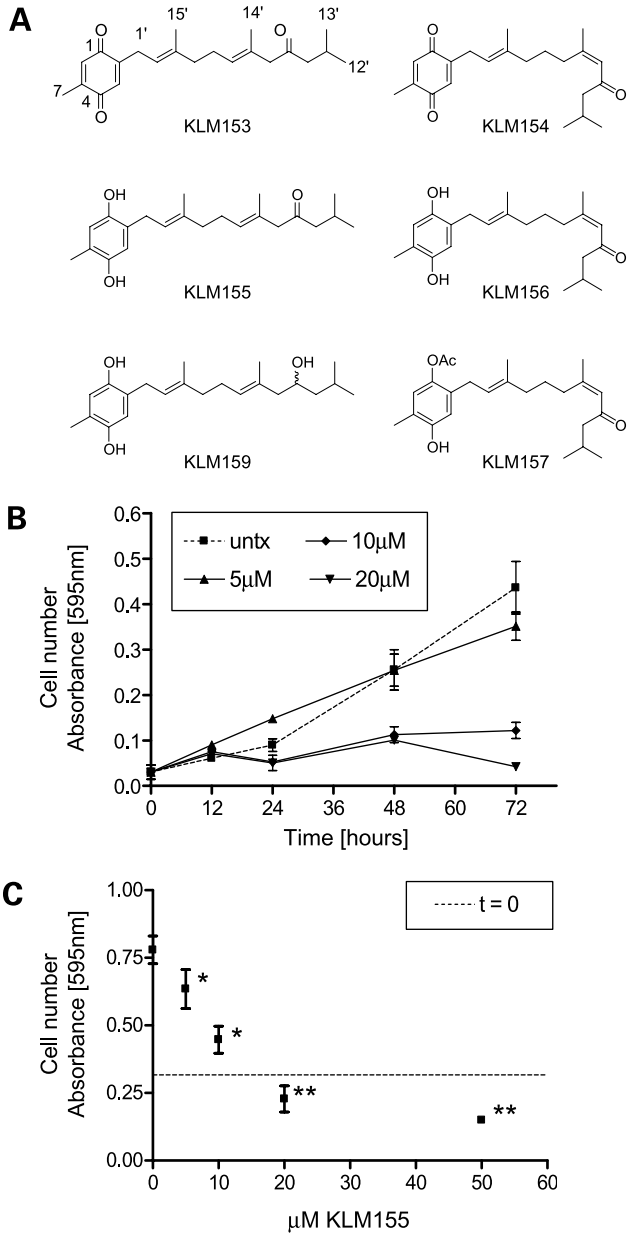

Figure 1. **A,** chemical structures of the compounds used in this study. **B,** effect of KLM155 on WHCO1 cell growth at three different concentrations, with cell number measured using the MTT kit. **C,** measurement of cell death compared with initial number of cells. WHCO1 cells were grown for 48 h (after an initial settling period of 24 h) in the presence of various concentrations of KLM155. Cell number was measured using the MTT kit. *, $P < 0.01$; **, $P < 0.001$. untx, untreated.

Table 1. IC_{50} values for each compound against the esophageal cancer cell line WHCO1

Compound	IC_{50} (μmol/L)	95% Confidence interval
KLM153	37.9	37.7–38.0
KLM154	83.3	82.1–84.5
KLM155	9.5	9.4–9.5
KLM156	12.9	12.5–13.3
KLM157	42.7	42.6–42.7
KLM159	32.7	32.5–33.0
cisplatin	16.5	13.5–20.3

NOTE: Cells were treated with a range of concentrations of each compound, and final cell number was determined using the MTT assay.

at least twice. Analysis was done using GraphPad Prism4 software, from a log-dose response curve to obtain log(IC_{50}). IC_{50} results are presented as the mean of 2 or 3 independent experiments with the 95% confidence intervals.

P values were calculated using Student's paired two-tailed *t* test.

Results

Treatment with Triprenyl Toluquinones and Toluhydroquinones Induces Cell Death in Cultured Human Cancer Cells

As part of our ongoing screening program (9–13), to identify potential lead compounds for use in the treatment of esophageal cancer, we tested six quinone-related compounds (KLM153–KLM157, KLM159; Fig. 1A) isolated from the nudibranch *L. millecra* (17) for cytotoxic activity against the esophageal cancer cell line WHCO1. Initial results from a crystal violet assay indicated that these compounds were active, with all causing ≥95% mortality after 48 h at 50 μg/mL. At 1 μg/mL, a slight increase in cell number was observed with some compounds (data not shown).

After the initial, promising results in the screening assay, these compounds were evaluated for their cytotoxic activity using the MTT assay to determine IC_{50} values (Table 1). Whereas the structures of these compounds are very similar, slight changes in substitution pattern on the ring or geometry of the double bonds in the side chain seemed to alter activity, with the most active compounds being those with a nonesterified hydroquinone nucleus (e.g., KLM155 and KLM156) with activity similar to cisplatin (16.5 μmol/L; ref. 12). The most active compound (KLM155) was evaluated against a range of cell lines, including esophageal cancer cell lines WHCO1 and WHCO6, cervical cancer cell lines ME180 and SiHa, and the benign breast epithelial line MCF12A as a control (Table 2). KLM155 displayed cytotoxicity against most of the cell lines tested, with the exception of the cervical cancer cell line SiHa.

Cell growth (Fig. 1B) and death (Fig. 1C) were evaluated with or without treatment to determine whether the reduction in cell number seen in screening was due to a cytotoxic or cytostatic effect. Whereas lower concentrations of KLM155 served only to slow cell growth (decrease cellular proliferation), higher concentrations clearly decreased cell number to levels below that measured at the time of treatment (indicated by the dotted line; Fig. 1C). The cytotoxic effect measured by MTT was associated with an altered morphology in treated cells, including cell rounding and membrane blebbing (data not shown).

Cell Death Induced by the Toluhydroquinone KLM155 is Associated with a Cell Cycle Block and Apoptosis

Considering the rounded cell morphology observed in cells treated with KLM155, cell cycle analysis was done to determine the effect of KLM155 on the cell cycle. Treatment with KLM155 at 20 μmol/L led to an increase in the G_2 population which persisted to 48 h (Fig. 2A). This was accompanied by a decrease in cell number of 51% at 24 h and 82% at 48 h.

We assessed the ability of KLM155 to induce apoptosis in WHCO1 cells by measuring the activity of caspase-3/caspase-7. Little apoptosis was observed at the lower concentrations with apoptosis levels at 20 μmol/L increasing to almost twice of that seen in untreated cells at 24 h ($P < 0.001$; Fig. 2B). The induction of apoptosis was confirmed using a flow cytometric approach using a fluorescently labeled antibody to activated caspase-3 (Fig. 2C) and was similar to that observed for doxorubicin-treated cells. The lack of a sub-G_1 peak of apoptotic cells in the cell cycle analysis is most likely due to the extended processing of cells for this assay (multiple washes and spins), during which this population may have been lost. We confirmed that the decrease in cell number seen was not due to necrosis by assessing levels of necrosis using the CytoTox-ONE homogeneous membrane integrity assay and showed no significant increase in necrosis (Fig. 2D).

Toluquinones and Toluhydroquinones Generate ROS in Cultured Cells, and ROS Generation Is Proportional to Cell Death

We hypothesized that the family of compounds discussed here act by generating ROS based on their structures. Our initial screening and activity results confirmed this hypothesis in several ways, with the increased growth of WHCO1 cells seen at low concentrations typical of treatment with a ROS-producing compound (21) and the activity variation with structure indicating the possible involvement of an autooxidative process for the hydroquinones (22). The compounds

Table 2. IC_{50} values for KLM155 against the esophageal cancer cell lines WHCO1 and WHCO6, the nonmalignant breast epithelial cell line MCF12, and the cervical carcinoma cell lines ME180 and SiHa

Cell line	IC_{50} (μmol/L)	95% Confidence interval
WHCO1	9.5	9.4–9.5
WHCO6	5.8	5.6–6.0
MCF12	32.0	31.6–32.3
ME180	33.9	33.7–34.1
SiHa	>150	

NOTE: Cells were treated with a range of concentrations of each compound, and final cell number was determined using the MTT assay.

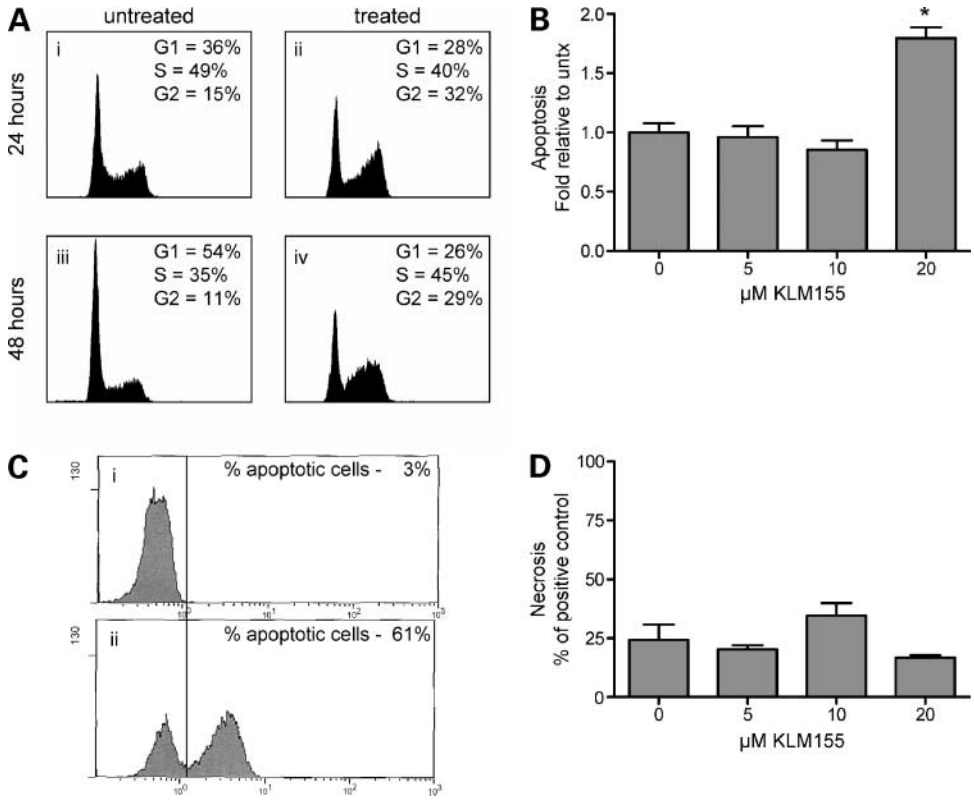

Figure 2. **A,** effect of KLM155 on cell cycle. WHCO1 cells were untreated (*i, iii*) or treated with 20 μmol/L KLM155 (*ii, iv*) for 24 h (*i, ii*) or 48 h (*iii, iv*), harvested by trypsinization, and processed for cell cycle analysis. Cell cycle profiles were analyzed using ModFit 3. **B,** induction of apoptosis by KLM155. WHCO1 cells were treated with various concentrations of KLM155 for 24 h. The cells were then processed to measure levels of active caspase-3/caspase-7 using the Caspase-Glo kit. *Columns,* mean; *bars,* SD ($n = 4$; *, $P < 0.001$). **C,** induction of apoptosis by KLM155. WHCO1 cells were untreated (*i*) or treated with 20 μmol/L KLM155 for 24 h (*ii*). The cells were then processed to measure levels of activated caspase-3 using a flow cytometry approach. **D,** induction of necrosis by KLM155. WHCO1 cells were treated with various concentrations of KLM155 for 24 h. Levels of necrosis were assessed using the CytoTox-ONE homogeneous membrane integrity assay (Promega G7890) and expressed as percentage of a positive (complete cell lysis) control. Similar results were obtained at 3-h, 6-h, and 12-h treatment.

were assessed for their ability to generate ROS in WHCO1 cells using the fluorescent probe DCF-DA. ROS induction (3.3-fold above untreated) was observed for KLM155 at 20 μmol/L ($P < 0.001$), but not at 5 μmol/L, and only a slight (1.3-fold) increase was observed at 10 μmol/L ($P < 0.05$; Fig. 3A). ROS production occurred within 15 min of treatment and increased steadily over 2 h (Fig. 3B). When the production of ROS in WHCO1 cells treated with 20 μmol/L of each compound was compared with the IC_{50} values obtained for this cell line, a linear relationship between the two was identified (Pearson's correlation $r = -0.818$, $P = 0.025$; Fig. 3C). This in particular suggests that the cytotoxic activity of these compounds is directly linked to their ability to produce ROS.

Treatment with Toluhydroquinone KLM155 Results in Activation of Several Mitogen-Activated Protein Kinase Signaling Molecules

The production of ROS in cells is often associated with the activation of mitogen-activated protein kinase pathways, e.g., JNK, ERK, and p38 (21, 23). We evaluated levels of phosphorylated p38, phosphorylated ERK, phosphorylated JNK, and phosphorylated c-Jun in treated cells at 6 and 24 h posttreatment (Fig. 4A).

Phosphorylated ERK levels were increased in a concentration-dependent manner at both time points. A slight induction of phosphorylated p38 was seen after treatment, and phosphorylated JNK levels did not increase except at the highest concentration, where a slight increase was seen, and phosphorylated c-Jun levels increased substantially at the highest concentration tested, but not at lower concentrations.

As expected, total ERK and total p38 levels were not altered. However, total JNK levels increased at 20 μmol/L KLM155 at 6 h and total c-Jun levels increased in a dose-dependent manner at both time points.

Because levels of phosphorylated c-Jun corresponded with ROS production and apoptosis induction, we further characterized the role of c-Jun/AP1 in toluhydroquinone-induced cell death using a model system available in our laboratory. CaSki cells are known to express high levels of AP1. We have available a CaSki cell line stably transfected with a doxycyclin-inducible dominant negative TAM67 construct. TAM67 is a c-Jun mutant lacking amino acids 3 to 122, removing the transactivating domain. TAM67 dimerises with wild-type c-Jun, but because it lacks the transactivation domain, the dimers comprising c-Jun and

TAM67 are unable to transcriptionally activate genes (19, 20). This cell line (referred to from here on as TAM67), together with the parental cell line (CaSki), was used to evaluate the role of c-Jun/AP1 in cellular response to treatment with the toluhydroquinone KLM155. Cell survival after treatment was increased in both the uninduced (82% survival) and induced (100% survival) TAM67 cell line compared with the parental line (53% survival; Fig. 4B). The increase in survival compared with the parental line is significant ($P < 0.01$) even in the case of uninduced TAM67 cells. The increased survival observed in the uninduced cells is due to the leaky expression of the TAM67 protein, as confirmed by Western blot analysis (Fig. 4B, bottom).

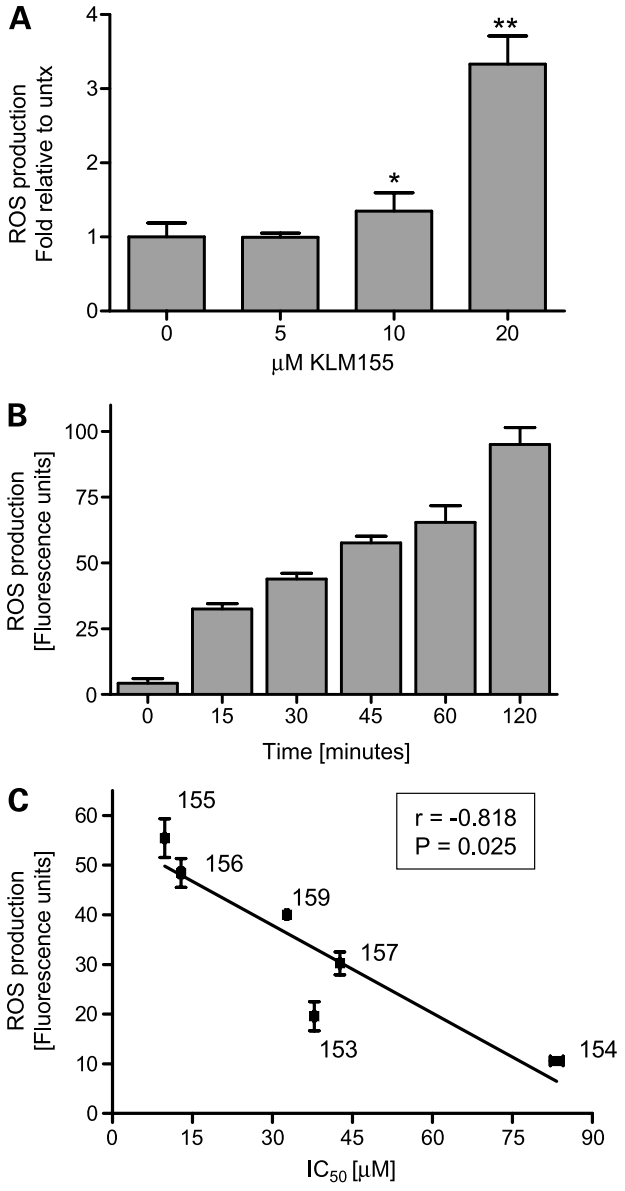

Figure 3. Induction of ROS in WHCO1 cells by the KLMs. Cells were treated with various concentrations of KLM155 for 1 h (**A**) or 20 μmol/L of KLM155 for the indicated periods (**B**) and treated with the different compounds at 20 μmol/L for 1 h (**C**). Cells were then harvested using trypsinization, stained using DCF-DA, and processed on a flow cytometer. **A,** *, $P < 0.05$; **, $P < 0.001$.

ROS Scavengers and a JNK Inhibitor Blocked KLM155-Induced Apoptosis

To test whether the cell death observed was mediated via production of ROS, we treated cells in the presence and absence of the ROS scavengers Trolox and butylated hydroxyanisol and JNK inhibitor II and assessed the cells for apoptosis (Fig. 4C) and survival (Fig. 4D).

When ROS scavengers were added to cells before treatment with KLM155, a 73% (Trolox, $P < 0.01$) and 66% (butylated hydroxyanisol, $P < 0.05$) reduction in caspase-3 activity induced by KLM155 was observed (Fig. 4C), and treated cells survived better (Fig. 4D). The JNK inhibitor did not have as clear an effect as it decreased levels of apoptosis (Fig. 4C) but did not significantly increase cell survival (Fig. 4D).

Discussion

This paper describes the anticancer activities of a family of novel compounds isolated from the nudibranch *L. millecra* collected from Algoa Bay, South Africa (17). Compounds KLM155 and KLM156 of this family of triprenylquinones and triprenylhydroquinones (Fig. 1) displayed moderate activity against cultured esophageal cancer cells, with IC_{50} values of 9.8 μmol/L and 12.9 μmol/L, respectively.

The ability of quinone and hydroquinone structures to act as ROS producers, as well as their more traditionally accepted role as ROS scavengers has been well-documented (22, 24). The ability of these compounds to inhibit proliferation in esophageal cancer cells was directly associated with the ability of these compounds to generate ROS. Firstly, we were able to directly measure ROS production in cells treated with these agents. Secondly, there was a strong inverse correlation between the IC_{50} values of the compounds tested and ROS production. And lastly, treatment of cells with the ROS scavengers butylated hydroxyanisol and Trolox reduced the extent of apoptosis caused by treatment with KLM155 (Fig. 4). Compelling evidence in the literature shows that ROS plays a central role in the antiproliferative activity of other agents that have potential as anticancer agents, including (*a*) 4-HPR in head and neck squamous carcinoma cell lines (25), (*b*) diallyl disulfide in neuroblastoma cells (26), (*c*) paclitaxel in T24 urothelial carcinoma cell lines (27), and (*d*) hetero-arotinoids in head and neck squamous cell carcinoma cell lines (28).

Our observation that ROS production is a relatively early event (within 15 min) is consistent with other reports that show early ROS production in cells treated with a variety of compounds that block cell growth and induce apoptosis through ROS-mediated pathways (25, 26). Oxidative stress is known to trigger a variety of responses in cells reflecting,

among others, the cell type studied, the level of ROS produced, and the duration of ROS exposure. ROS is known to damage various cellular components, and the cellular response to this damage is generally to attempt repair (frequently associated with a cell cycle block), followed by cell death if the damage is irreparable. The cellular events we observe after treatment with KLM155, namely cell cycle arrest and apoptosis, are characteristics of ROS-induced cell death (26, 27).

Several cellular signaling pathways may play a role in ROS-mediated cell death; among these are the mitogen-activated protein kinase pathways including Ras/Raf/MAP/ERK kinase/ERK, p38, and stress-activated protein kinase/JNK. We evaluated the levels of key molecules in these signaling pathways and identified a slight dose-dependent increase of phosphorylated p38.

Both phosphorylated ERK and c-Jun levels increased in a dose-dependent manner. However, phosphorylated c-Jun and phosphorylated JNK levels increased at only the highest concentration of KLM155 tested (20 μmol/L). The increase in these proteins correlated with the levels of ROS produced (Fig. 3A) and levels of caspase activation (Fig. 2B).

The role of ROS in activating JNK (an important upstream activator of c-Jun) through the inactivation of

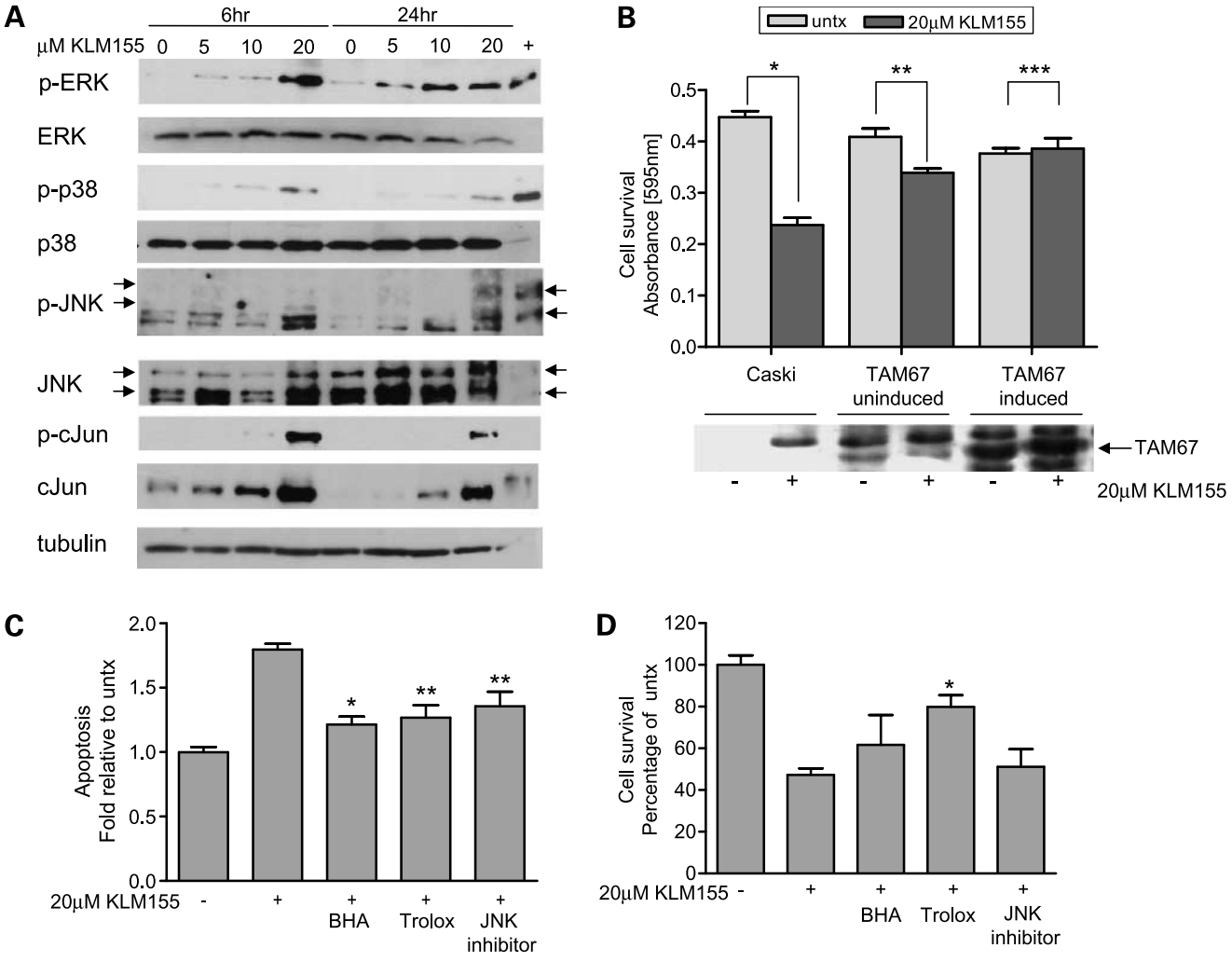

Figure 4. **A,** signaling events after treatment with KLM155. WHCO1 cells were treated with various concentrations of KLM155 for 6 h and 24 h. Protein lysates were prepared, separated by SDS-PAGE, transferred, and immunoblotted to detect the indicated proteins. A positive control for phosphorylated p38 (*p-p38*; UV-treated cells) was included (*last lane, marked +*). **B,** effect of TAM67 on cell survival in response to treatment with KLM155. Parental CaSki cells and a stably transfected cell line expressing the dominant negative AP1 construct TAM67 (uninduced and induced with 2000 ng/mL doxycyclin) were treated with 20 μmol/L KLM155. Cells were then either evaluated to determine the remaining number of cells (expressed as percentage of untreated for each experimental condition), or protein lysate was collected to determine levels of TAM67 (lower panel). **C,** effect of inhibitors on KLM155 induced apoptosis. Cells were pretreated for 2 h with the indicated inhibitors, then treated for 24 h with or without 20 μmol/L KLM155. They were then processed to assess levels of apoptosis using the Caspase-Glo kit (Promega G8090; data are expressed at fold increase relative to untreated). **D,** effect of inhibitors on cell survival after treatment with KLM155. Cells were pretreated for 2 h with the indicated inhibitors, then treated for a further 24 h with or without 20 μmol/L KLM155. Cells were then processed with the MTT kit to assess remaining number of cells (data are expressed as percentage of untreated for each inhibitor). **B,** *, $P < 0.01$; **, $P < 0.05$; ***, $P = 0.5$. **C,** *, $P < 0.01$; **, $P < 0.05$. **D,** *, $P < 0.001$.

endogenous JNK inhibitors has already been documented (29, 30), providing a plausible pathway for the induction of c-Jun observed here. Our results strongly implicated JNK/c-Jun signaling in mediating KLM155-induced apoptosis, considering the induction of c-Jun subsequent to treatment with KLM155 and the observation that the JNK inhibitor abrogated KLM155-induced apoptosis. It was quite intriguing that while the JNK inhibitor significantly blocked the apoptosis induced by KLM155, this inhibitor had no significant effect on the reduction in cell number caused by KLM155 (Fig. 4C and D). This should be considered in the context of the results observed for Trolox, which blocked apoptosis to the same extent as the JNK inhibitor but was associated with a 20% reduction in cell number in response to treatment with KLM155. Presumably, the block in apoptosis caused by the JNK inhibitor occurs despite the ROS-induced cellular damage inflicted by treatment of cells with KLM155. This level of cellular damage is sufficient to induce a cell cycle block as shown in Fig. 2A, effectively preventing cellular proliferation. The severely damaged cells may also self destruct through nonapoptotic pathways if denied access to apoptosis, as previously described (31). Of course, the ability of Trolox and butylated hydroxyanisol to block both apoptosis and the reduction in cell number caused by treatment with KLM155 reflects the proximal site of action of these ROS scavengers, allowing them to protect cells from extensive ROS-induced damage and thus precluding the requirement for apoptosis or alternative cell death pathways.

Cancer cells generally are exposed to much higher levels of oxidative stress than normal cells (32). This is based on direct measurements of ROS levels in tumor tissues (33), accumulation of oxidative products in tumor tissue (34), and the presence of oxidized DNA products in the urine of cancer patients (35). Of particular interest for this study are the elevated levels of superoxide dismutase measured in squamous cell carcinomas of the esophagus relative to normal tissues (36), suggesting that esophageal tumor tissues are also under increased oxidative stress. As a result of the constant assault of oxidative stress, cancer cells have an impaired ability to deal with oxidative stress (relative to normal cells), rendering them sensitive to additional oxidative challenges. This diminished ability of cancer cells to mount an effective response to further oxidative challenges may represent a critical therapeutic window that could be exploited to develop more selective anticancer agents. The central role of ROS in mediating the cytotoxic activity of the family of triprenylquinones and triprenylhydroquinones described here underscores the value of this novel family of compounds as potential lead chemotherapeutic agents for further structure/function analysis.

In fact, the close structural similarity of this family of compounds isolated from *L. millecra* allows us to make some tentative structure/activity observations. Comparing the effect of the side chain on activity, the all-trans conformation confers greater activity than the trans-cis conformation in both cases (KLM153 compared with KLM154; KLM155 compared with KLM156). The substitution pattern at the 1 and 4 positions yields varying activity with (KLM156 > KLM157 > KLM154: -OH > -OAc > =O) which corresponds with previous observations (37). Although the cell lines used in this paper differ from those evaluated by Li et al. (37), this observation may be of use in rational drug design and is possibly linked to the electron-donating ability of the hydroxyl compared with the carbonyl.

The strong correlation between the levels of ROS produced by each of the compounds and their IC_{50} values and the structural similarity of the family of compounds described here provide an opportunity to further explore the structural elements that confer activity in these molecules. This study and others (9–11) support the hypothesis that marine benthic organisms from the coast of southern Africa represent a rich, untapped repository of novel and interesting compounds that may hold promise in the development of new chemotherapeutic agents.

Acknowledgments

PhD scholarships (C.E. Whibley) from National Research Foundation, Deutscher Akademischer Austauschdienst, and University of Cape Town and postdoctoral scholarships (R.A. Keyzers) from National Research Foundation and Rhodes University are gratefully acknowledged. Prof. M.I. Parker's (University of Cape Town) support for the project is appreciated.

References

1. Cragg GM, Newman DJ. Plants as a source of anti-cancer agents. J Ethnopharmacol 2005;100:72 – 9.

2. Newman DJ, Cragg GM. Marine natural products and related compounds in clinical and advanced preclinical trials. J Nat Prod 2004; 67:1216 – 38.

3. Andersen RJ, Williams DE. Pharmaceuticals from the Sea. In: Hester RE, Harrison RM, editors. Chemistry in the Marine Environment. Cambridge: RSC Press; 2000. p. 55 – 79.

4. Haefner B. Drugs from the deep: marine natural products as drug candidates. Drug Discov Today 2003;8:536 – 44.

5. Proksch P, Edrada-Ebel R, Ebel R. Drugs from the sea - opportunities and obstacles. Mar Drugs 2006;1:5 – 17.

6. Mayer AMS, Gustafson KR. Marine pharmacology in 2001-2: antitumour and cytotoxic compounds. Eur J Cancer 2004;40:2676 – 704.

7. Blunt JW, Copp BR, Munro MHG, Northcote PT, Prinsep MR. Marine natural products. Nat Prod Rep 2005;22:15 – 61.

8. Davies-Coleman MT. Bioactive Natural Products from Southern African Marine Invertebrates. In: Atta-ur-Rahman, editor. Studies in Natural Product Chemistry (Bioactive Natural Products Part L). Amsterdam: Elsevier; 2005.

9. Davies-Coleman MT, Dzeha TM, Gray CA, et al. Isolation of homodolastatin 16, a new cyclic depsipeptide from a Kenyan collection of Lyngbya majuscula. J Nat Prod 2003;66:712 – 5.

10. Keyzers RA, Arendse CE, Hendricks DT, Samaai T, Davies-Coleman MT. Makaluvic acids from the South African Iatrunculid sponge Strongylodesma aliwaliensis. J Nat Prod 2005;68:506 – 10.

11. Knott MG, Mkwananzi H, Arendse CE, Hendricks DT, Bolton JJ, Beukes DR. Plocoralides A-C, polyhalogenated monoterpenes from the marine alga Plocamium corallorhiza. Phytochemistry 2005;66:1108 – 12.

12. Rajput J, Moss JR, Hutton AT, Hendricks DT, Arendse CE, Imrie C. Synthesis, characterization and cytotoxicity of some palladium(II), platinum(II), rhodium(I) and iridium(I) complexes of ferrocenylpyridine and related ligands. Crystal and molecular structure of *trans*-dichlorobis(3-ferrocenylpyridine)palladium(II). J Organomet Chem 2004;689:1553 – 68.

13. Whibley CE, Keyzers RA, Soper AG, Davies-Coleman MT, Samaai T, Hendricks DT. Antioesophageal cancer activity from Southern African marine organisms. Ann N Y Acad Sci 2005;1056:405 – 12.

14. Mqoqi N, Kellerr P, Madhoo J, Sitas F; National Cancer Registry of South Africa. Incidence and geographical distribution of histologically

diagnosed cancer in South Africa, 1996 – 1997. Johannesburg: National Cancer Registry of South Africa, South African Institute for Medical Research; 2003.

15. Lordick F, Stein HJ, Peschel C, Siewert JR. Neoadjuvant therapy for oesophagogastric cancer. Br J Surg 2004;91:540 – 51.

16. Enzinger PC, Mayer RJ. Esophageal cancer. N Engl J Med 2003;349: 2241 – 52.

17. McPhail KL, Davies-Coleman MT, Starmer J. Sequestered chemistry of the Arminacean nudibranch Leminda millecra in Algoa Bay, South Africa. J Nat Prod 2001;64:1183 – 90.

18. Veale RB, Thornley AL. Increased Single Class Low-Affinity Egf Receptors Expressed by Human Esophageal Squamous Carcinoma Cell-Lines. S Afr J Sci 1989;85:375 – 9.

19. Hennigan RF, Stambrook PJ. Dominant negative c-jun inhibits activation of the cyclin D1 and cyclin E kinase complexes. Mol Biol Cell 2001;12:2352 – 63.

20. Freemerman AJ, Turner AJ, Birrer MJ, Szabo E, Valerie K, Grant S. Role of c-jun in human myeloid leukemia cell apoptosis induced by pharmacological inhibitors of protein kinase C. Mol Pharmacol 1996;49: 788 – 95.

21. Ruiz-Ramos R, Cebrian ME, Garrido E. Benzoquinone activates the ERK/MAPK signaling pathway via ROS production in HL-60 cells. Toxicology 2005;209:279 – 87.

22. Watanabe N, Forman HJ. Autoxidation of extracellular hydroquinones is a causative event for the cytotoxicity of menadione and DMNQ in A549-S cells. Arch Biochem Biophys 2003;411:145 – 57.

23. Seanor KL, Cross JV, Nguyen SM, Yan M, Templeton DJ. Reactive quinones differentially regulate SAPK/JNK and p38/mHOG stress kinases. Antioxid Redox Signal 2003;5:103 – 13.

24. Asche C. Antitumour quinones. Mini Rev Med Chem 2005;5:449 – 67.

25. Kim HJ, Chakravarti N, Oridate N, Choe C, Claret FX, Lotan R. N-(4-Hydroxyphenyl)retinamide-induced apoptosis triggered by reactive oxygen species is mediated by activation of MAPKs in head and neck squamous carcinoma cells. Oncogene 2006;25:2785 – 94.

26. Filomeni G, Aquilano K, Rotilio G, Ciriolo MR. Reactive oxygen species-dependent c-Jun NH2-terminal kinase/c-Jun signaling cascade mediates neuroblastoma cell death induced by diallyl disulfide. Cancer Res 2003;63:5940 – 9.

27. Ramanathan B, Jan KY, Chen CH, Hour TC, Yu HJ, Pu YS. Resistance to paclitaxel is proportional to cellular total antioxidant capacity. Cancer Res 2005;65:8455 – 60.

28. Chun KH, Benbrook DM, Berlin KD, Hong WK, Lotan R. The synthetic heteroarotinoid SHetA2 induces apoptosis in squamous carcinoma cells through a receptor-independent and mitochondria-dependent pathway. Cancer Res 2003;63:3826 – 32.

29. Chen YR, Shrivastava A, Tan TH. Down-regulation of the c-Jun N-terminal kinase (JNK) phosphatase M3/6 and activation of JNK by hydrogen peroxide and pyrrolidine dithiocarbamate. Oncogene 2001;20: 367 – 74.

30. Bernardini S, Bernassola F, Cortese C, et al. Modulation of GST P1 – 1 activity by polymerization during apoptosis. J Cell Biochem 2000;77: 645 – 53.

31. Zhang XD, Wu JJ, Gillespie S, Borrow J, Hersey P. Human melanoma cells selected for resistance to apoptosis by prolonged exposure to tumor necrosis factor-related apoptosis-inducing ligand are more vulnerable to necrotic cell death induced by cisplatin. Clin Cancer Res 2006;12:1355 – 64.

32. Pelicano H, Carney D, Huang P. ROS stress in cancer cells and therapeutic implications. Drug Resist Updat 2004;7:97 – 110.

33. Zhou Y, Hileman EO, Plunkett W, Keating MJ, Huang P. Free radical stress in chronic lymphocytic leukemia cells and its role in cellular sensitivity to ROS-generating anticancer agents. Blood 2003;101: 4098 – 104.

34. Senthil K, Aranganathan S, Nalini N. Evidence of oxidative stress in the circulation of ovarian cancer patients. Clin Chim Acta 2004;339: 27 – 32.

35. Chiou CC, Chang PY, Chan EC, Wu TL, Tsao KC, Wu JT. Urinary 8-hydroxydeoxyguanosine and its analogs as DNA marker of oxidative stress: development of an ELISA and measurement in both bladder and prostate cancers. Clin Chim Acta 2003;334:87 – 94.

36. Janssen AM, Bosman CB, van Duijn W, et al. Superoxide dismutases in gastric and esophageal cancer and the prognostic impact in gastric cancer. Clin Cancer Res 2000;6:3183 – 92.

37. Li XF, Choi HD, Kang JS, Lee CO, Son BW. New polyoxygenated farnesylcyclohexenones, deacetoxyyanuthone A and its hydro derivative from the marine-derived fungus Penicillium sp. J Nat Prod 2003;66: 1499 – 500.

Molecular Cancer Therapeutics

Reactive oxygen species mediated apoptosis of esophageal cancer cells induced by marine triprenyl toluquinones and toluhydroquinones

Catherine E. Whibley, Kerry L. McPhail, Robert A. Keyzers, et al.

Mol Cancer Ther 2007;6:2535-2543.